Modeling and Simulation for Additive Manufacturing

National Academy of Engineering

U.S. National Committee on Theoretical and Applied Mechanics (USNC/TAM)

Workshop on Predictive Theoretical and Computational Approaches for Additive Manufacturing

10/7-9/2015

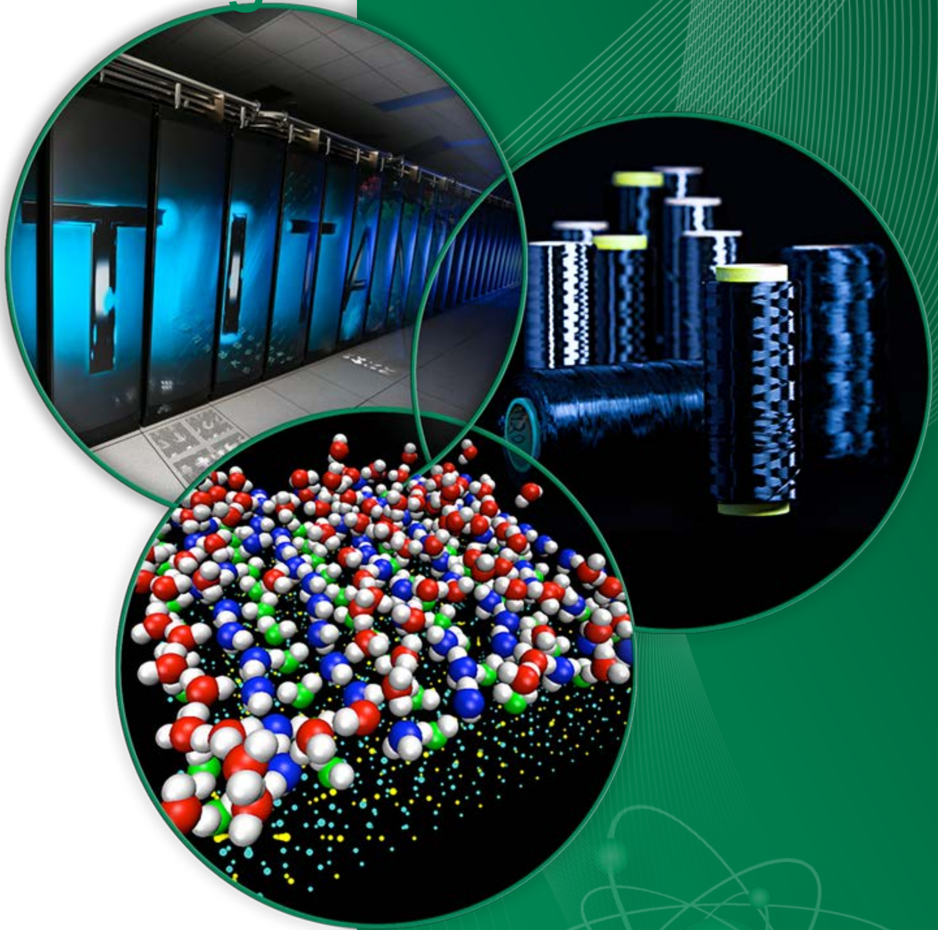

John A. Turner
Group Leader
Computational Engineering and Energy Sciences
Sudarsanam Suresh Babu
Governor’s Chair
University of Tennessee, Knoxville
Narendran Raghavan
University of Tennessee, Knoxville

Outline

- Application example
- Challenges of metal additive manufacturing processes
- Powder
  - Properties
  - Melting
- Mesoscale
- Engineering scale
  - Relationship between process parameters and microstructure

Which armor would you rather be behind?

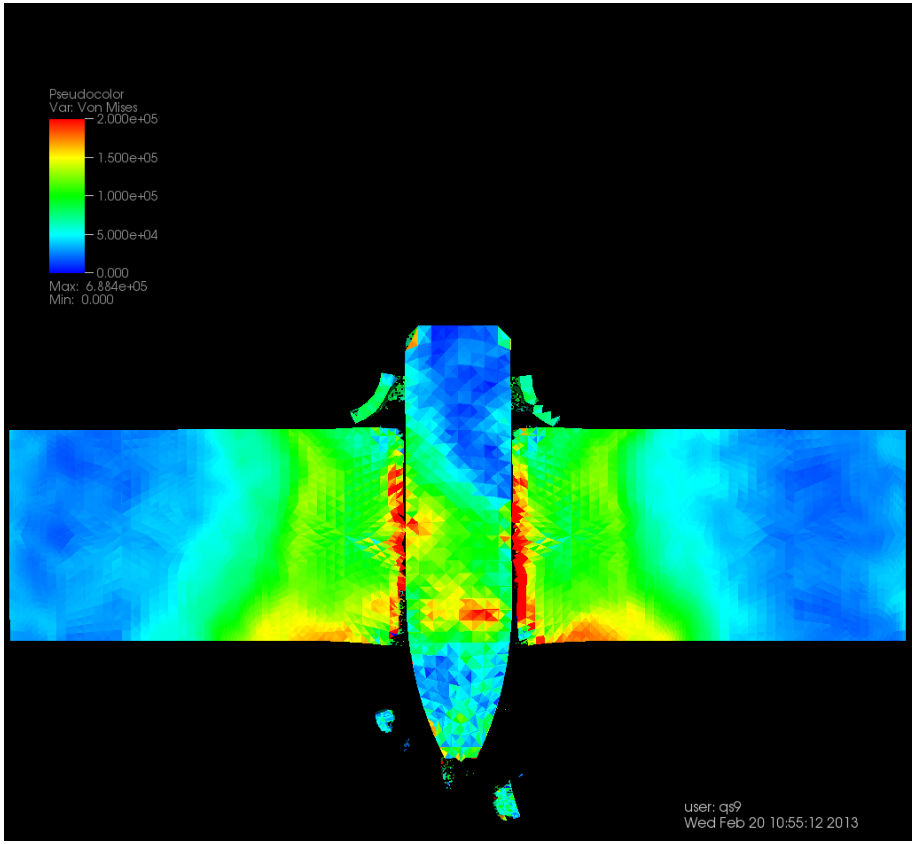

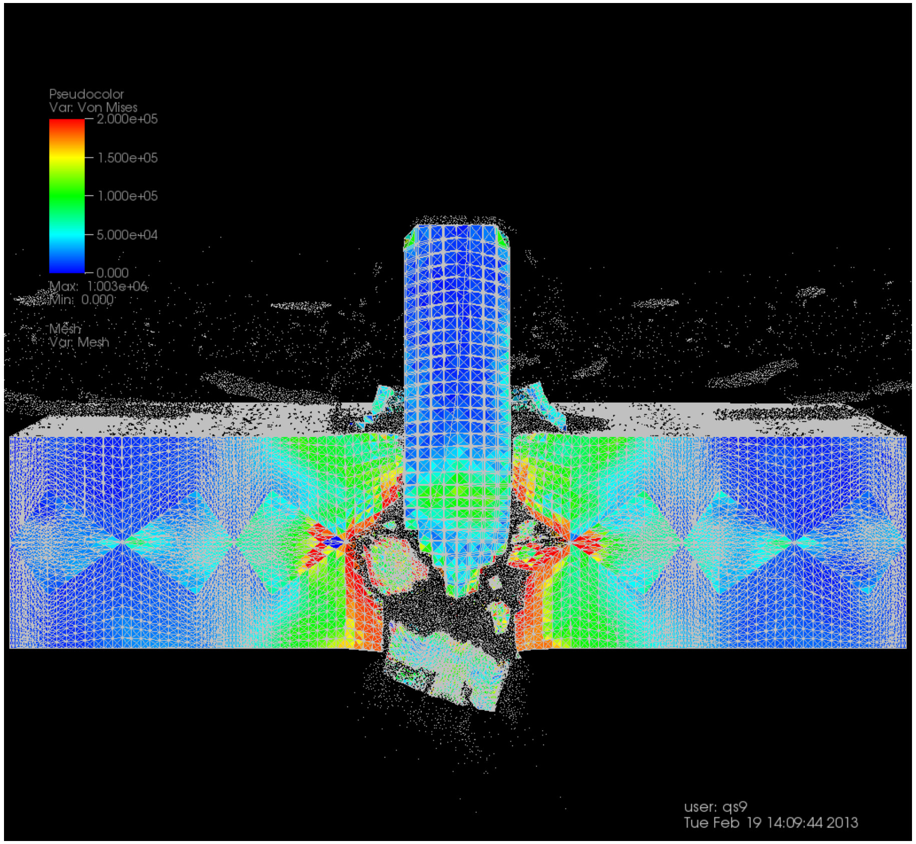

Movies replaced by still images for distribution

Computer Modeling of Impact - FEM

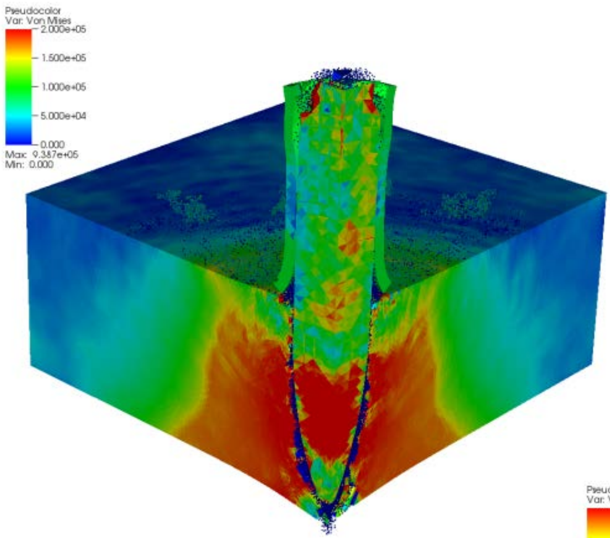

a) Monolithic Ti-6Al-4V

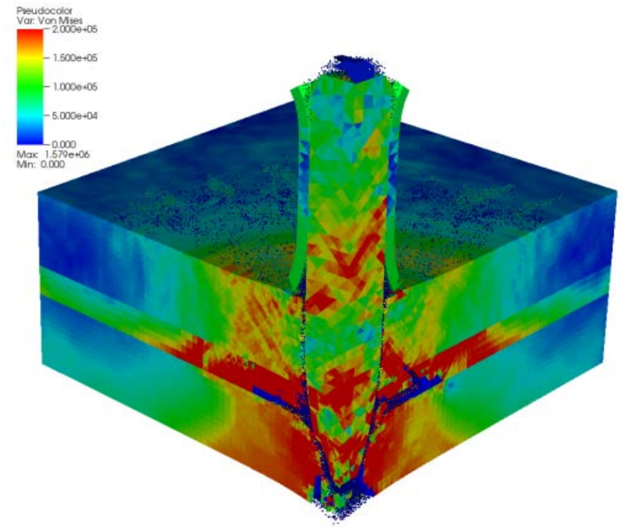

b) Ti-6Al-4V with laminar hard core

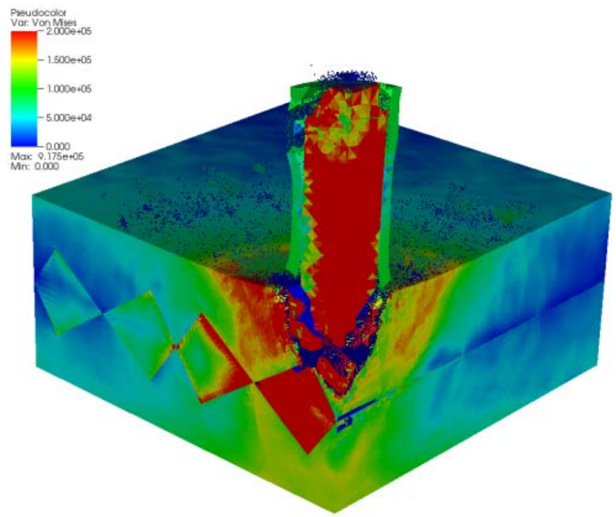

c) Ti-6Al-4V with geometrically complex hard core

The complex shape armor fractures the penetrator and therefore has better ballistic efficiency than the layered armor with the same volume fractions of materials.

Hard core total volume is equal in b) and c)

3D Finite Element Modeling (FEM) of Additively-Manufactured Armor/Anti-Armor (better performance, lower weight)

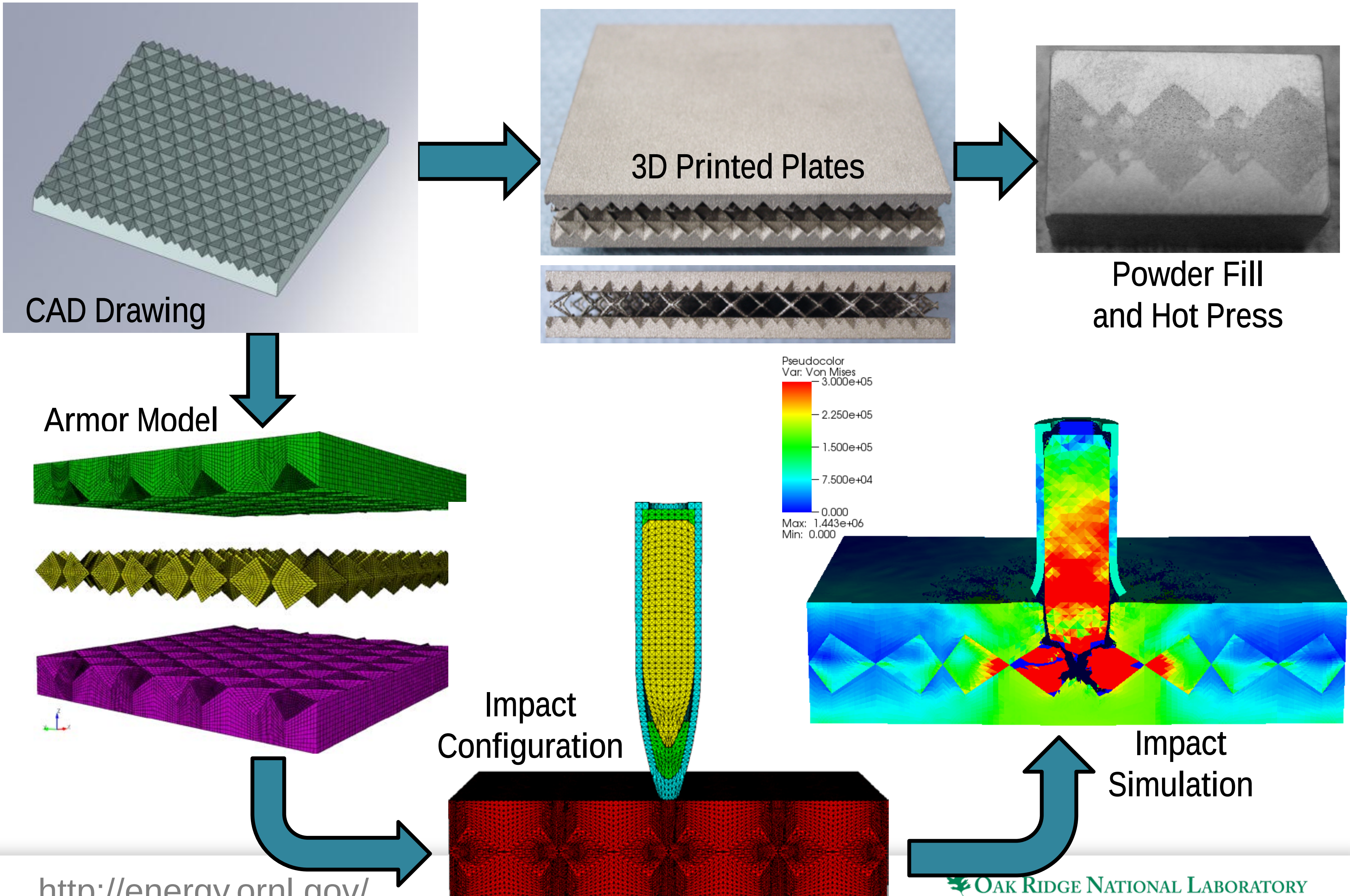

Multiple AM technologies

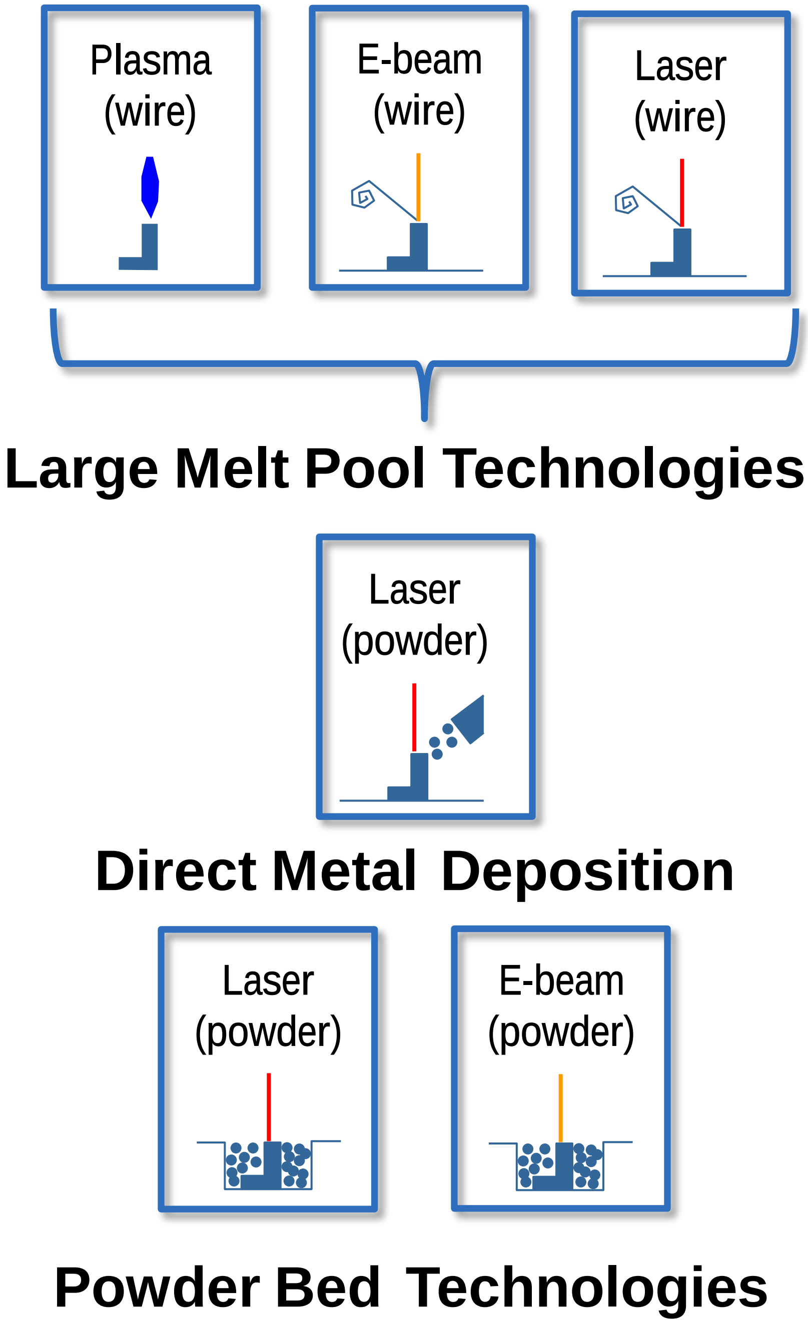

Physical processes are similar

- Energy Deposition
- Melting & Powder Addition
- Evaporation & Condensation
- Heat & Mass Transfer
- Solidification
- Solid-State Phase Transformation
- Repeated Heating and Cooling
- Complex Geometries

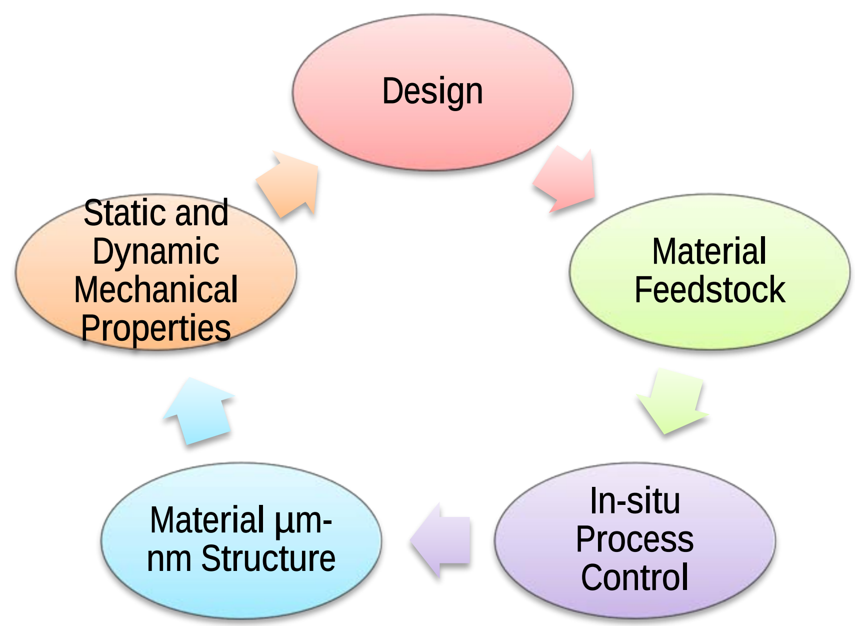

Complex coupled multiscale physics processes control additive manufacturing

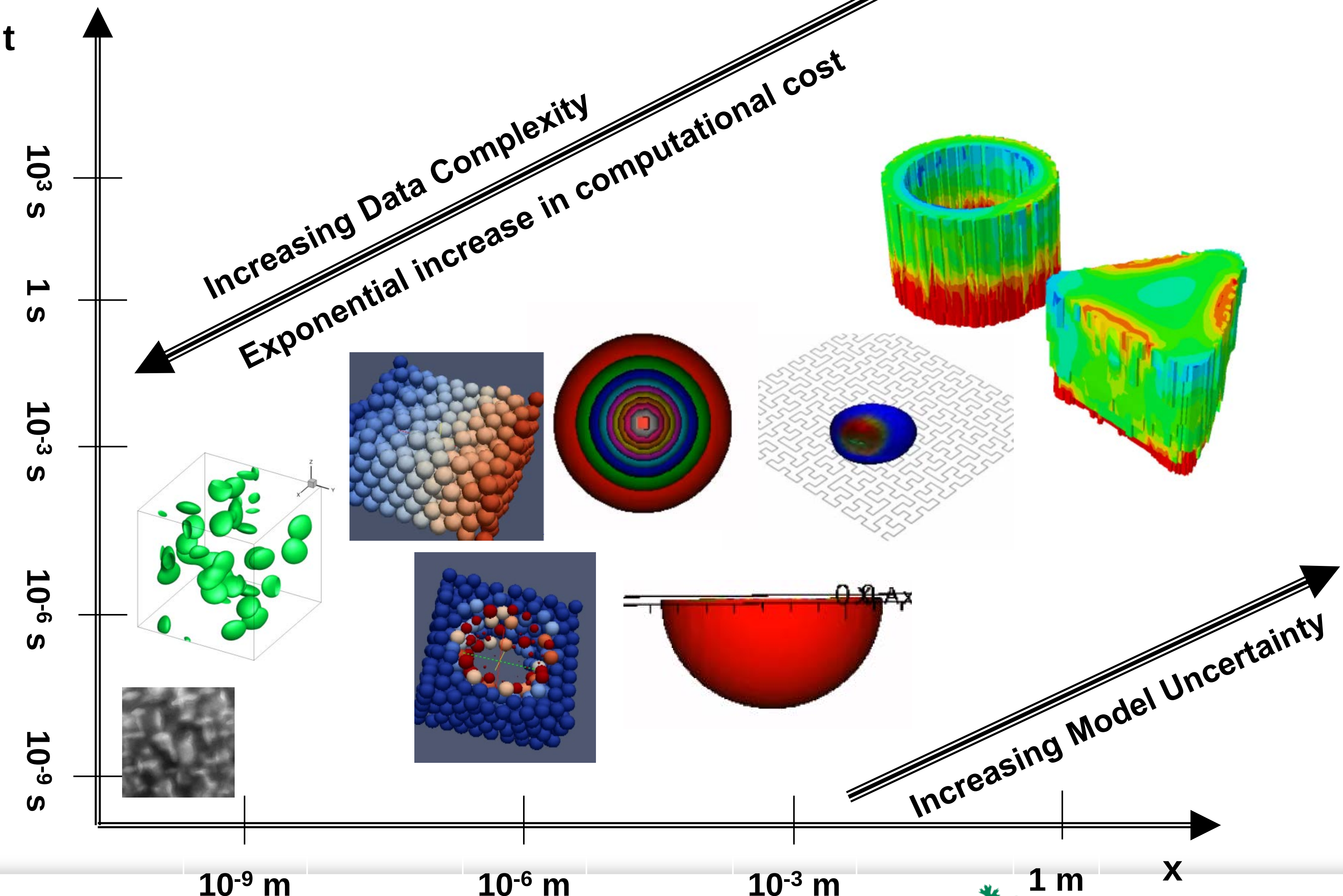

Multiple computational challenges must be addressed for AM.

- 1 m^3 ~ 10^{12} particles ~ 10^9 m of “weld” line (assuming 50μm particles) and build times of hours
  - Brute force approaches will fail
- Large temperature gradients, rapid heating and cooling
  - necessary / sufficient coupling between thermomechanics and melt/solidification
- Heterogeneous and multi-scale
  - resolution of energy sources and effective properties of powder for continuum simulations
- Path optimization
- Large number of parameters and missing understanding
  - key uncertainties and propagation of those uncertainties
- Validation is difficult as characterization is limited

A broad spectrum of computational science is required to fully realize the promise of additive manufacturing.

Energy Interaction with Porous Materials

Gas-Liquid-Solid Reactions

Rapid Melting, Solidification & Crystallography

Elastic / Plastic Strain Evolution

Solid-Solid Phase Transformation Under Thermomechanical Cycling

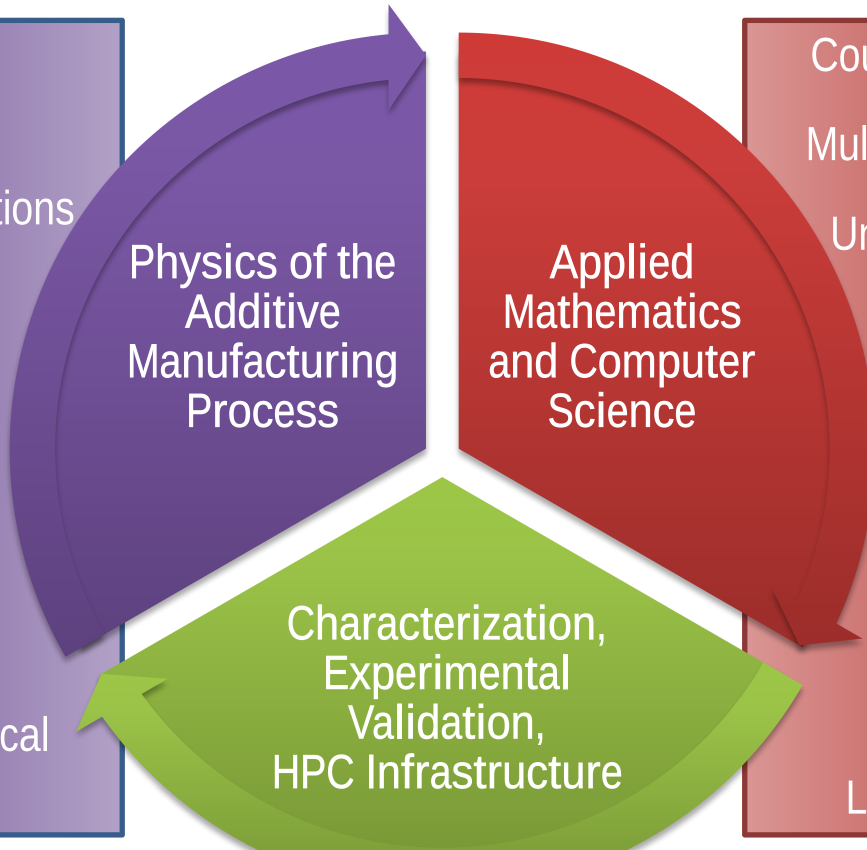

Coupled large-scale PDEs

Multiscale coupled physics

Uncertainty quantification and design under uncertainty

Risk analysis and decision making

Scalable software

Large-scale inverse problems

Large-scale optimization

In some cases, models, techniques, and capabilities in these areas exist for other applications, and can be brought to bear on challenges of AM.

Computational capability has increased at a relatively steady pace for decades.

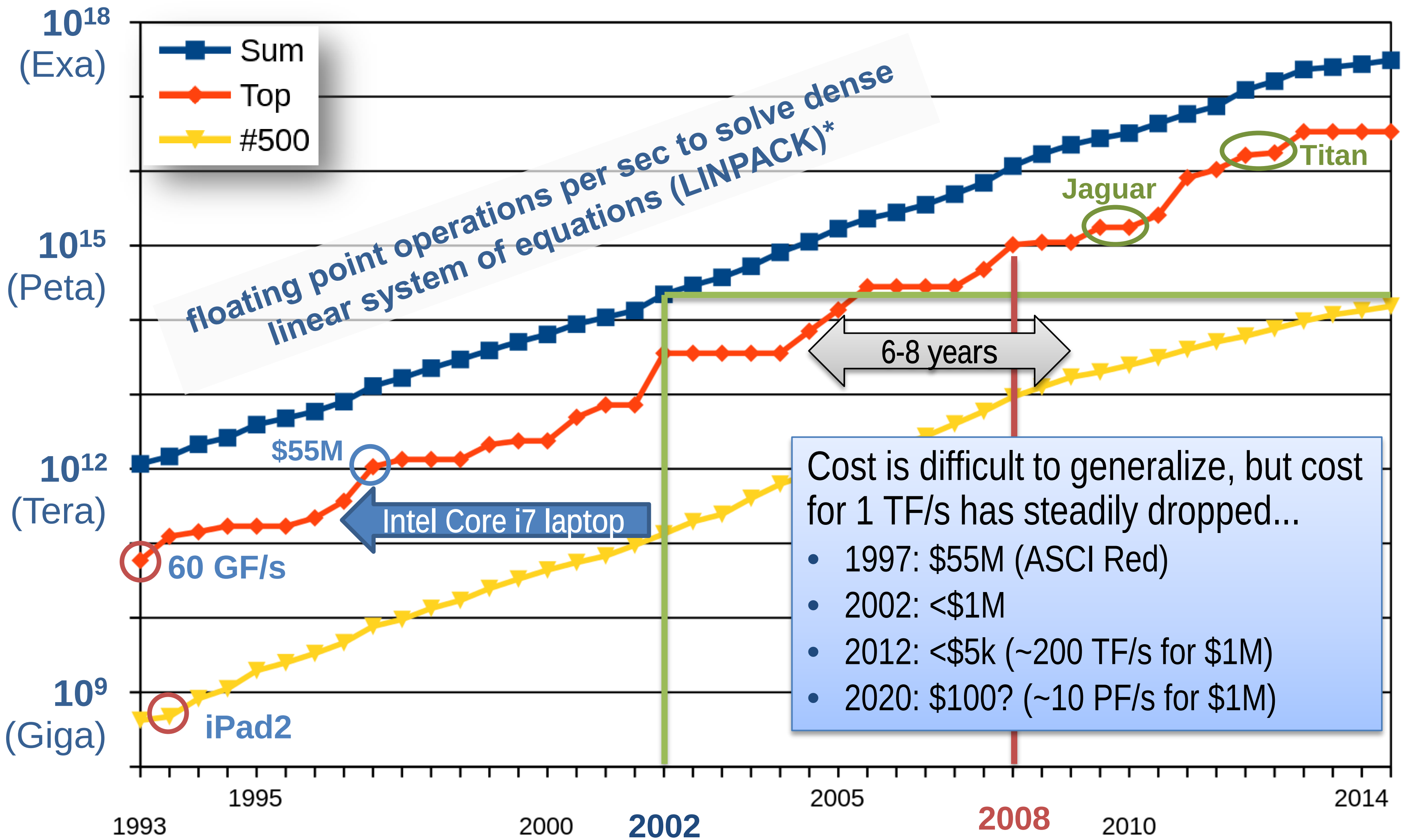

http://en.wikipedia.org/wiki/TOP500

What is the sensitivity of the SLM process to particle level variations?

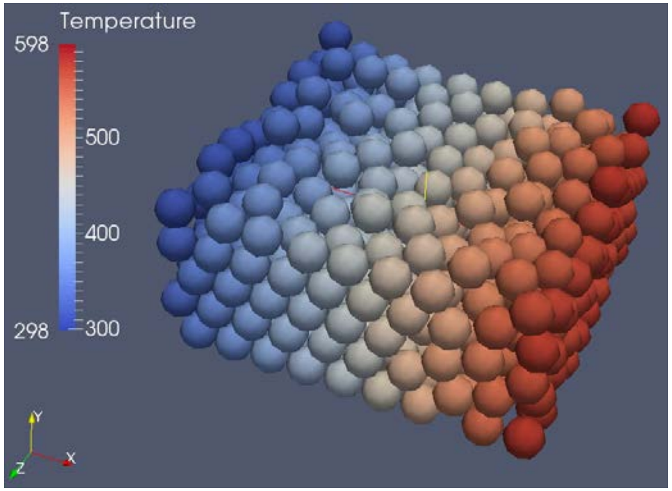

Movies replaced by still images for PDF

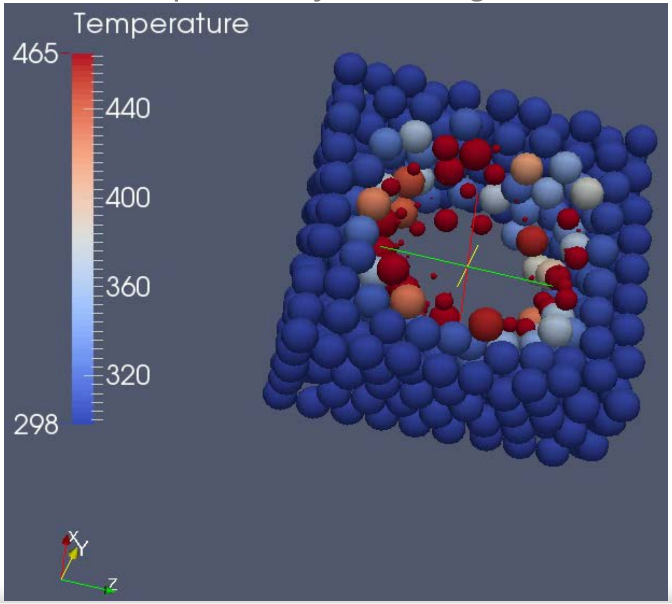

- Heat transfer in powders and packed beds
  - Granular dynamics that include heat transfer, melting, and solidification
  - Coating powders as we go forward for using AM for alloys?
  - Spatiotemporal distribution of multi-size and multi-material powders
- These simulations are for SLM of Nylon/Ti64 powder bed
- These detailed simulations are being used to get effective properties such as
  - conductivity
  - laser penetration and distribution
  - effective melting/solidification properties

All simulations in MFIX with Dan Moser

Generating bed configurations

Avg. Size	Frac. Of Total
31.2 μm	0.119
44.6 μm	0.228
58 μm	0.310
71.4 μm	0.228
84.8 μm	0.119

Nylon-12 (25-92 μm)

Avg. Size	Frac. Of Total
50.5 μm	0.115
61.5 μm	0.230
72.5 μm	0.311
83.5 μm	0.230
94.5 μm	0.115

Ti64 (45-100 μm)

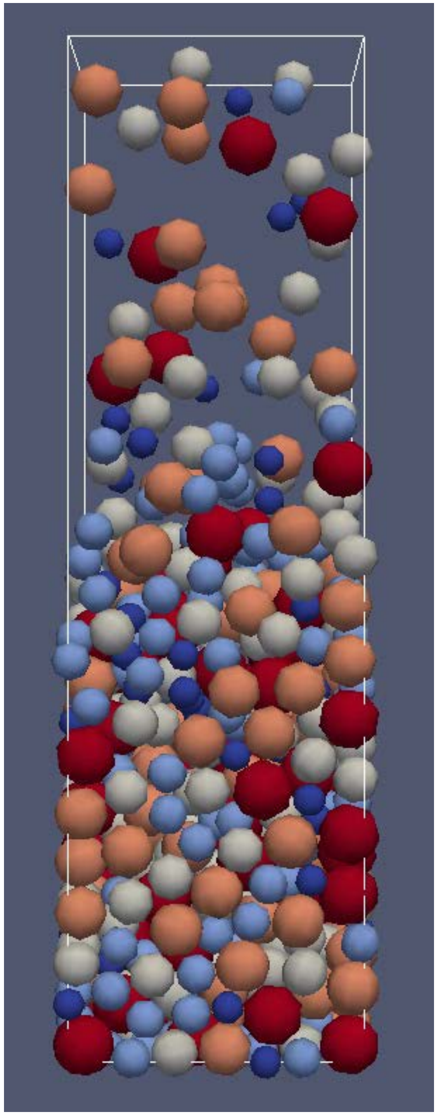

Generate loose-packed bed

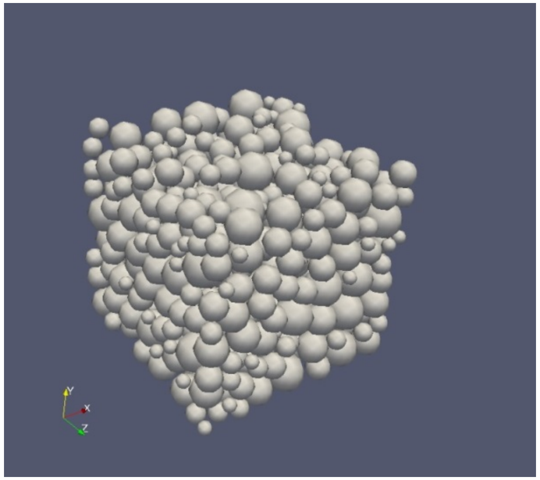

Nylon-12

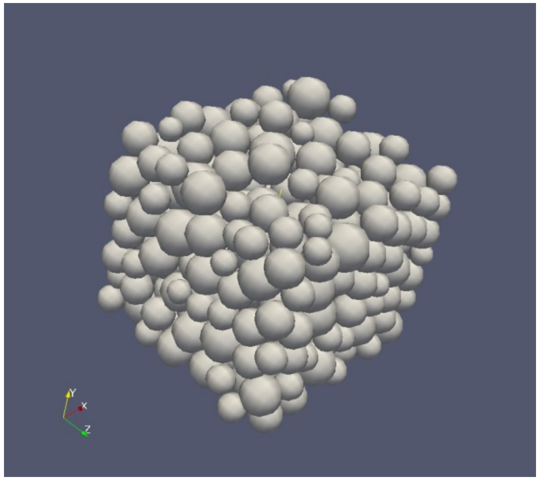

Ti64

Movie replaced by still image for distribution

Conductivity is calculated at using particle-particle conduction models

- Particle-particle contact conduction (R_c is contact radius):
  - $\dot{Q}_{pp}^{(i,j)} = \frac{4k_i k_j}{k_i + k_j} R_c (T_j - T_i)$
- Particle-fluid-particle conduction (l_{cond} is conduction distance, Λ mean free path of gas, and ac thermal accommodation coefficient)
  - $\dot{Q}_{pfp}^{(i,j)} = k_g (T_j - T_i) \int_{R_c}^{R_{min}} \frac{2\pi r}{l_{cond} + M} dr$
  - $M = \left[\frac{2 - ac_1}{ac_1} + \frac{2 - ac_2}{ac_2}\right] \frac{\gamma}{\gamma + 1} \frac{1}{Pr} \Lambda$
- Particle-particle radiation (view factors calculated using Monte-Carlo ray tracing)
  - $\dot{Q}_{rad}^{(i,j)} = \frac{\sigma (T_i^4 - T_j^4)}{\frac{1 - \varepsilon_i}{\varepsilon_i A_i} + \frac{1}{A_i F_{i \to j}} + \frac{1 - \varepsilon_j}{\varepsilon_j A_j}}$
- Particle temperatures are solved for that drive net heat transfer rates to 0. Conductivity can then be determined from heat flux from fixed temperature walls

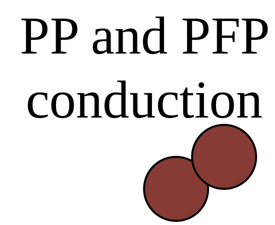

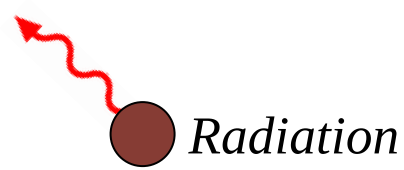

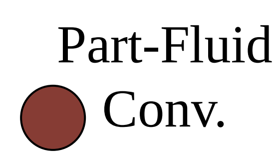

Powder conductivity is almost decoupled from bulk property

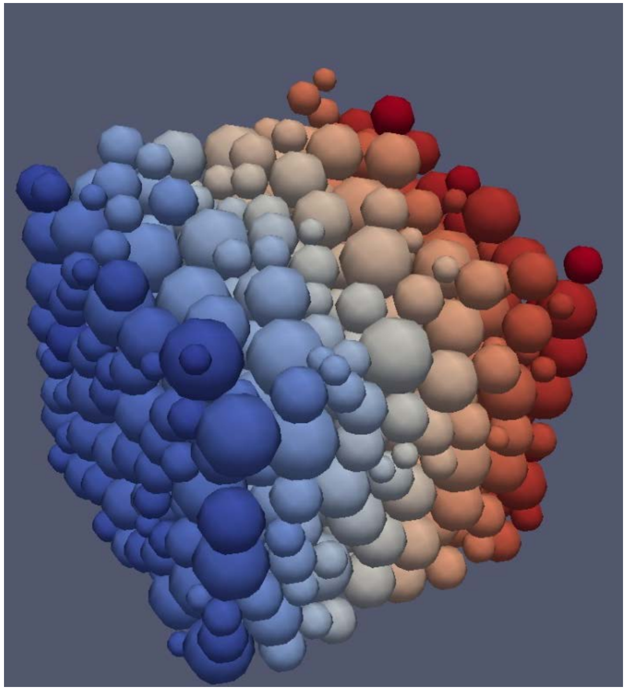

Steady state temperature distribution in powder bed (Nylon-12)

Input uncertainties and modeling errors dominate the uncertainty as compared to different packings.

Config #	# of Particles	Conductivity (W / mK)
1	565	0.1097
2	548	0.1111
3	543	0.1053
4	568	0.1167
5	556	0.1100
6	572	0.1068
7	579	0.1063

Nylon-12 @ 313K

Config #	# of Particles	Conductivity (W / mK)
1	306	0.2203
2	292	0.2184
3	319	0.2219
4	329	0.2246
5	325	0.2262
6	323	0.2348
7	297	0.2232

Ti64 @ 1400K

Compare to uncertainties for initial approximations of bulk properties

Original

Property	Symbol	Range
Effective Conductivity	k	0-0.27 W/m/°K
Effective Emissivity	ε	0.75-1
Extinction Coefficient	β	130-215 1/cm

Property	Symbol	Range
Effective Conductivity	k	0.093-0.122 W/m/°K
Effective Emissivity	ε	0.84-0.96
Extinction Coefficient	β	130-144 1/cm

Nylon-12

Original

Property	Symbol	Range
Effective Conductivity	k	0-19.5 W/m/°K
Effective Emissivity	ε	0.3-1
Extinction Coefficient	β	103-172 1/cm

Property	Symbol	Range
Effective Conductivity	k	0.182-0.262 W/m/°K
Effective Emissivity	ε	0.53-0.575
Extinction Coefficient	β	125-139 1/cm

Ti-64

Nylon calculation matches measurement for DuraForm powder at 40°C of 0.1 W/mK

Particle Melt Modeling

- Develop a relation for powder bed melt percentage as a function of laser power added
- Represent powder bed as spherical particles superimposed on a background mesh
- Use the discrete element model (DEM) in the multiphase code MFIX
- As DEM particles melt and shrink due to applied heat source, mass added to background mesh
- Particles beneath shielded (insulated)

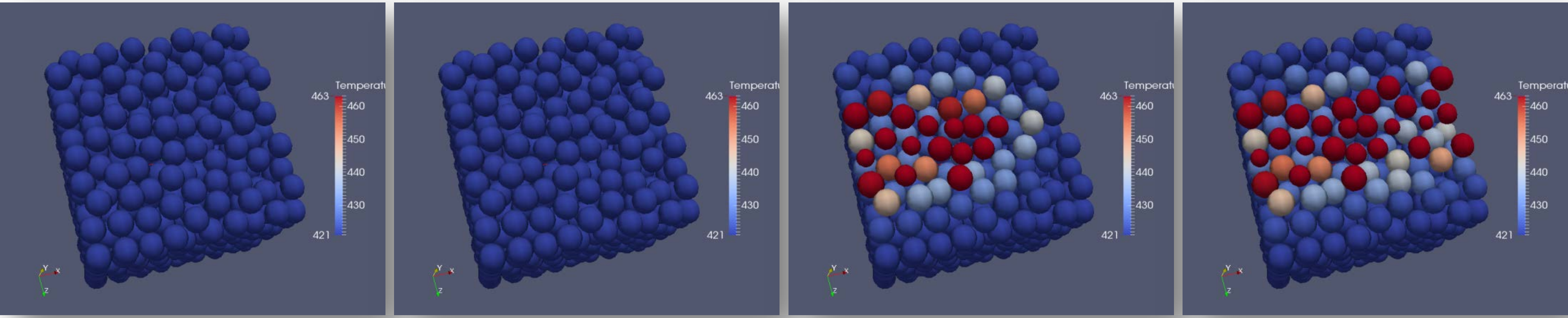

Phase Field Simulations used to understand microstructural evolution during LAM of Ti-6Al-4V

Features of Phase Field Model

- Fully integrated with system thermodynamics
- System energy includes contributions from anisotropic interfacial energy, and elastic energy due to transformation strains
- Governing equations solved using Fourier spectral method exploiting P3DFFT library in Titan (large runs with thousands of processors)
- Unique composite nucleation model that allows growth of specific variants assisted by local strain field

Fundamental question addressed

- Why do layer bands form during solid-state transformation of pre-solidified material?
  - Intra-granular nucleation of colony structure?

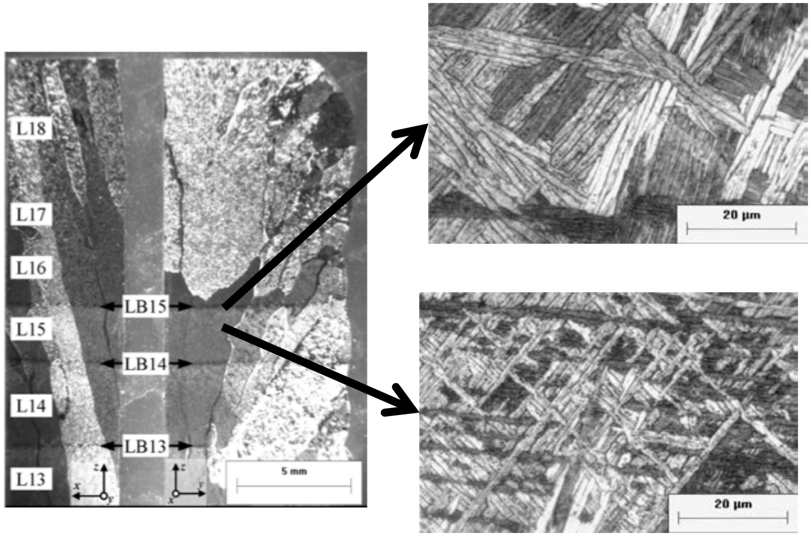

From Kelly and Kampe, 2004

Length scale of prior β grains much larger than packet size of colony

Nucleation rate identified as the main factor responsible for formation of colony structure

Parametric studies performed using phase field simulations

- Two levels of thermodynamic driving force: low (1000K) and high: 950K
- Two levels of nucleation rate: low (0.5 s^{-1}) and high (5 s^{-1})

Crucial Findings

- Low nucleation rate promotes colony when a new nucleus sees well developed strain field from a nearby variant
- High nucleation rate promotes basket weave when all nuclei see complex strain field due to multiple, evolving nuclei

Auto-catalytic colony nucleation

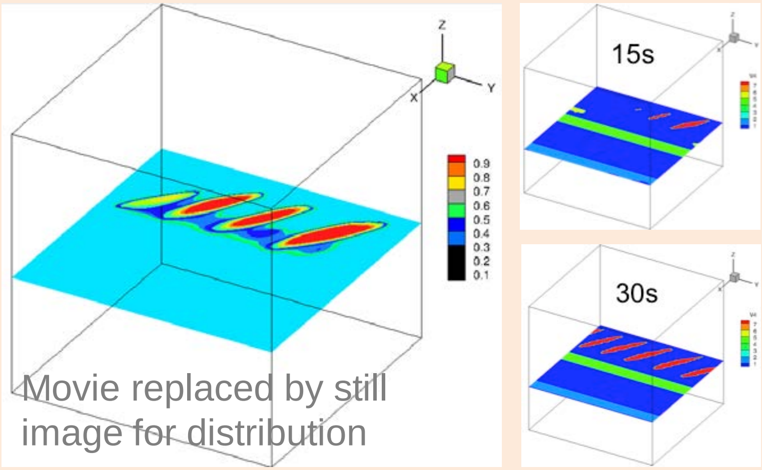

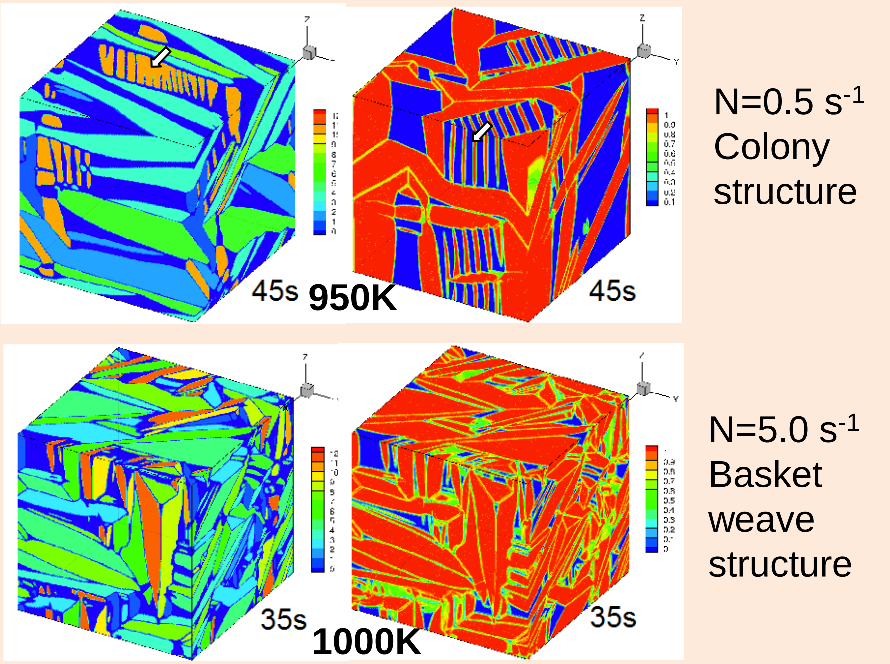

B. Radhakrishnan, S.B. Gorti and S.S. Babu, PTM 2015: International Conference on Solid-Solid Phase Transformations in Inorganic Materials, Whistler, Canada (Invited)

Overview of Electron beam Additive Manufacturing (Arcam®)

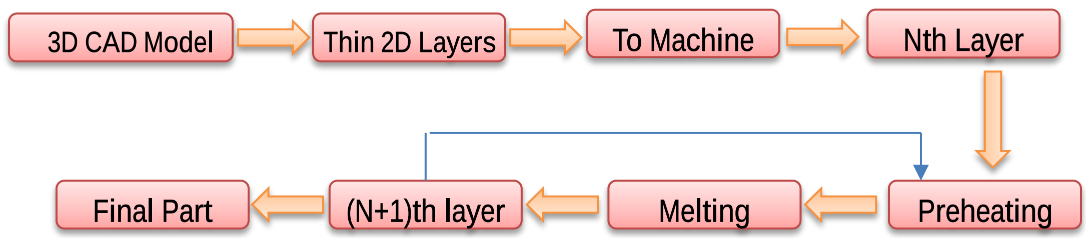

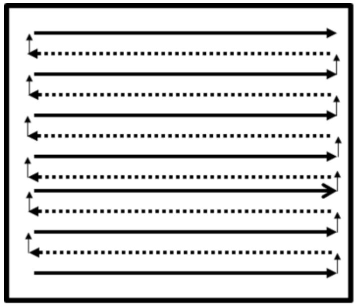

Conventional Raster Melt sequence

Microstructure manipulation of IN718 via additive manufacturing is not well understood. Always results in columnar grains oriented along the build direction (001)

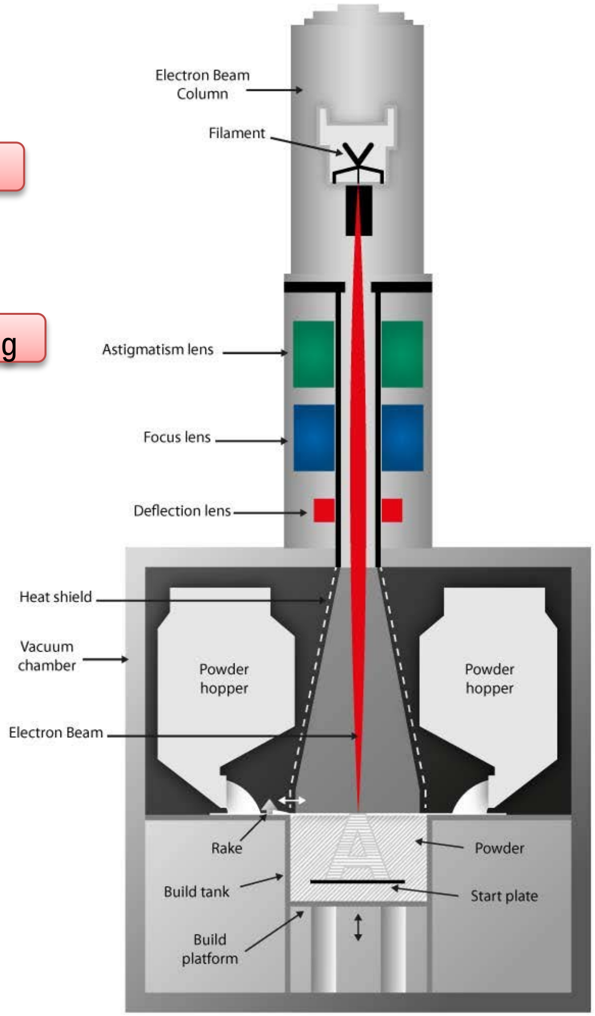

Source: http://www.arcam.com/technology/electron-beam-melting/hardware/

- Microstructure of the material plays significant role in determining the mechanical properties of final part
    - Directional vs Isotropic properties
- Feasibility of site specific microstructure control?

Macro-microscale melting/solidification

- Truchas was developed at LANL to model metal casting processes
  - Heat conduction, convection, and radiation (simple and view factors)
  - Incompressible, multi-material, free-surface fluid flow with VOF interface tracking
  - Multi-component species advection-diffusion
- Adapting at ORNL to AM applications
  - Different beam path sequences
  - Heat source distribution for EBM processes

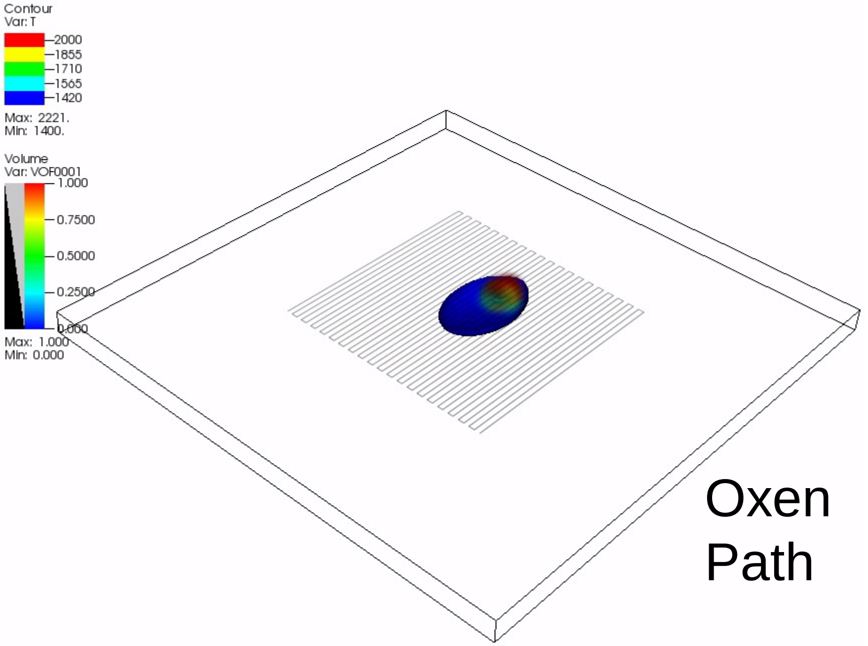

Movies replaced by still images for distribution

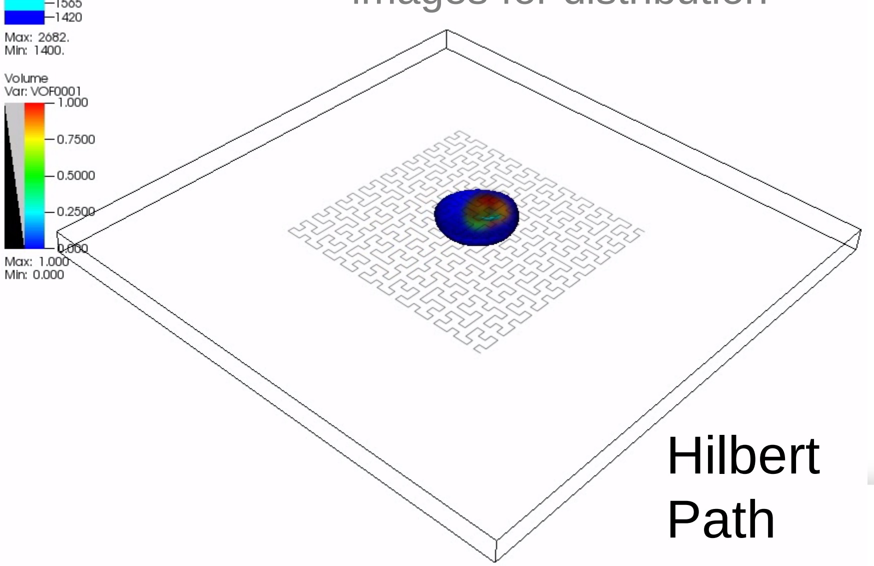

- Electron beam melting process (Arcam) and Inconel 718
- Beam velocity of 4 m/s and power of 2.4 kW, beam diameter and depth of 200 μm
- Over 10 different path sequences have been implemented and these can be dynamically varied with feedback

Spot melting and simulation

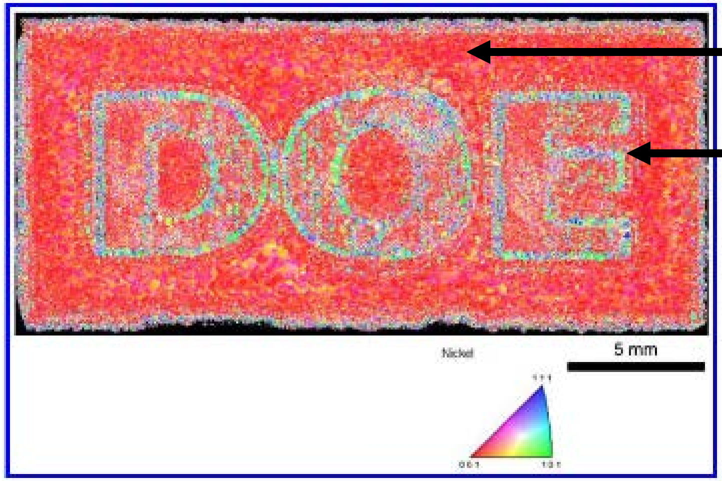

†

Conventional Raster Pattern

Spot Melt Pattern along the contour “DOE”

- CET in rapid solidification processes primarily controlled by
  - Thermal gradient at the liquid solid interface (G)
  - Velocity or growth rate of liquid-solid interface (R)
- Difficult to measure experimentally.
  - Spatial resolution (microns)
  - Temporal resolution required (milliseconds)
  - Thermal imaging camera cannot capture 3D data
- Truchas metal casting code
  - Developed at LANL for metal casting of nuclear materials.
  - Spatial domain can be split and allocated to multiple processors to reduce simulation time.

Spot melting can also reduce simulation time by isolation and avoiding complexity of raster pattern by reducing the length of melt pool

† Dehoff, R. R., Kirka, M. M., Sames, W. J., Bilheux, H., Tremsin, A. S., Lowe, L. E., & Babu, S. S. (2015). Site specific control of crystallographic grain orientation through electron beam additive manufacturing. *Materials Science and Technology*, *31*(8), 931-938.

Numerical Analysis of Spot Melting

Truchas Output:

- Spatiotemporal variation of temperature
  - 1-3 million nodes depending on problem size

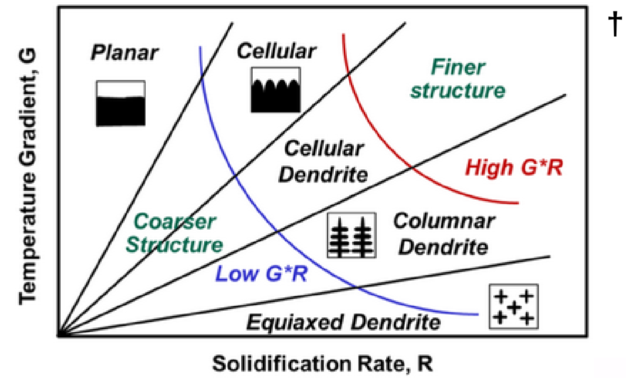

†

Post processing of Truchas Output:

- Resultant thermal Gradient at the liquid solid interface

$$G\left(\frac{K}{m}\right) = \sqrt{G_x^2 + G_y^2 + G_z^2}$$

- Velocity of liquid-solid interface

$$R\ (m/s) = \frac{Cooling\ Rate\quad (K/s)}{Thermal\ Gradient\quad (K/m)} = \frac{\left|\frac{dT}{dt}\right|}{\sqrt{G_x^2 + G_y^2 + G_z^2}}$$

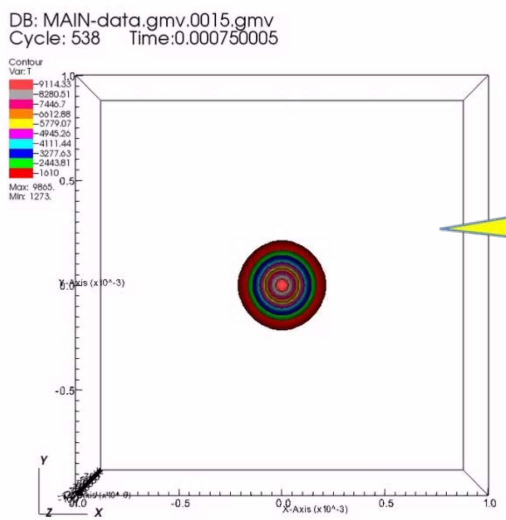

Melt pool Tracking

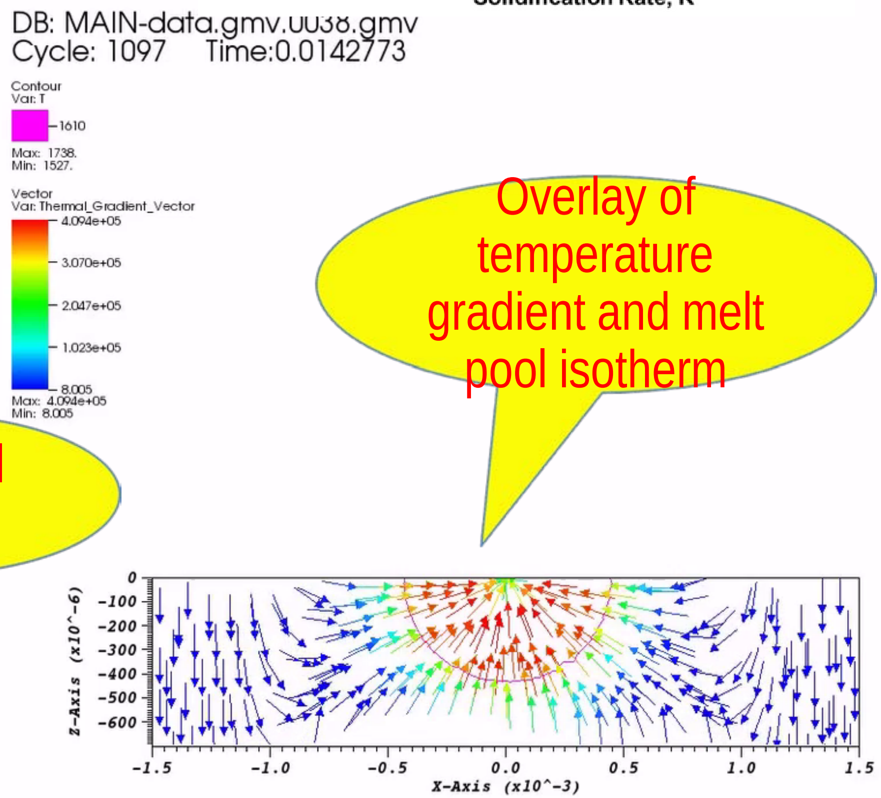

Overlay of temperature gradient and melt pool isotherm

† Lee, Y., Nordin, M., Babu, S. S., & Farson, D. F. (2014). Effect of Fluid Convection on Dendrite Arm Spacing in Laser Deposition. *Metallurgical and Materials Transactions B*, *45*(4), 1520-1529.

Movies replaced by still images for distribution

Spatio-Temporal Variation of G and R on Solidification Map

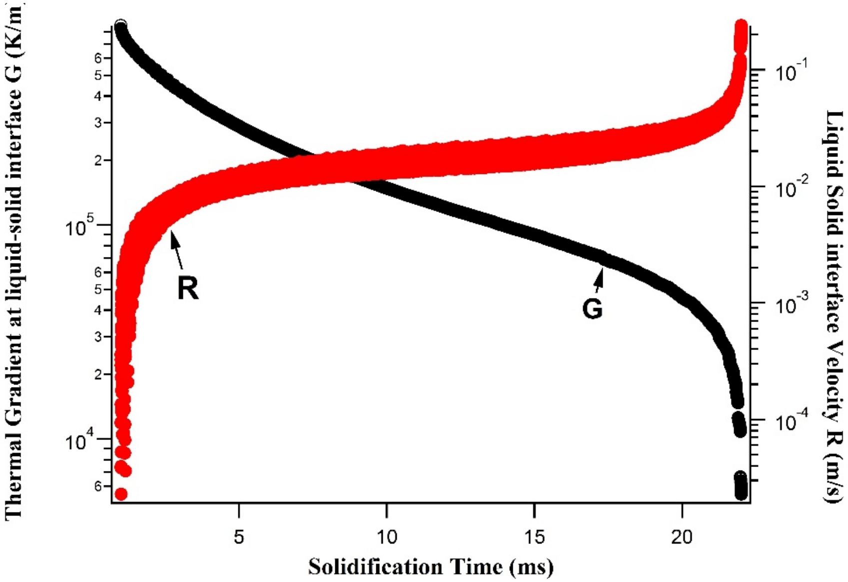

a) G and R as function of solidification time

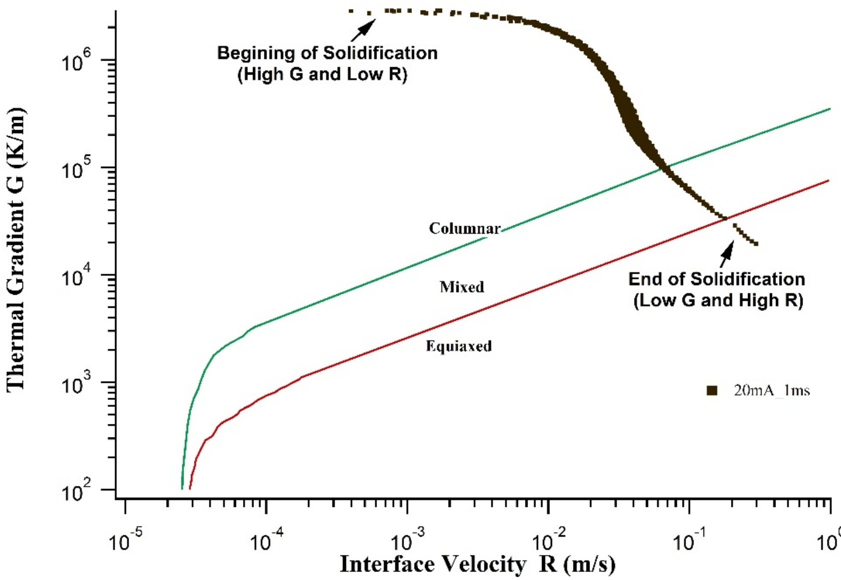

b) G vs R on IN718 Reference solidification map

Qualitative Effect of Process Parameters on G vs R

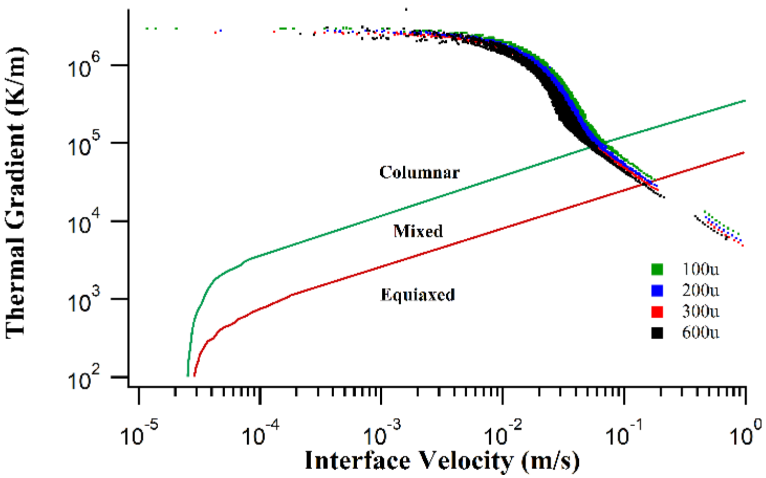

a) Beam Diameter

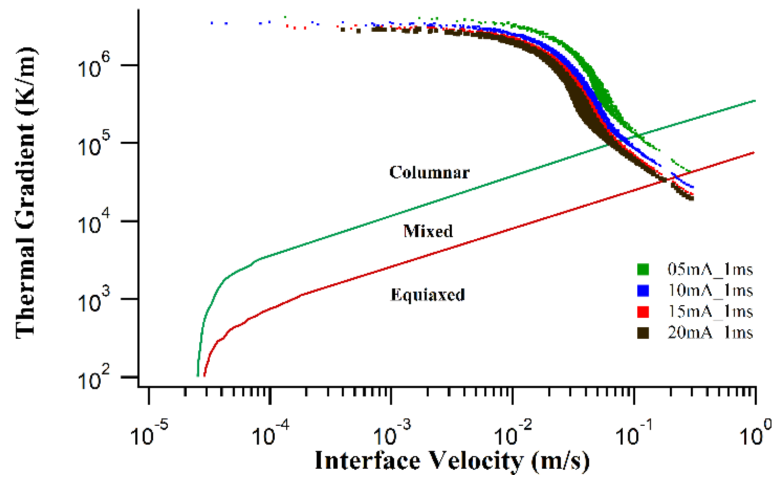

b) Beam Current

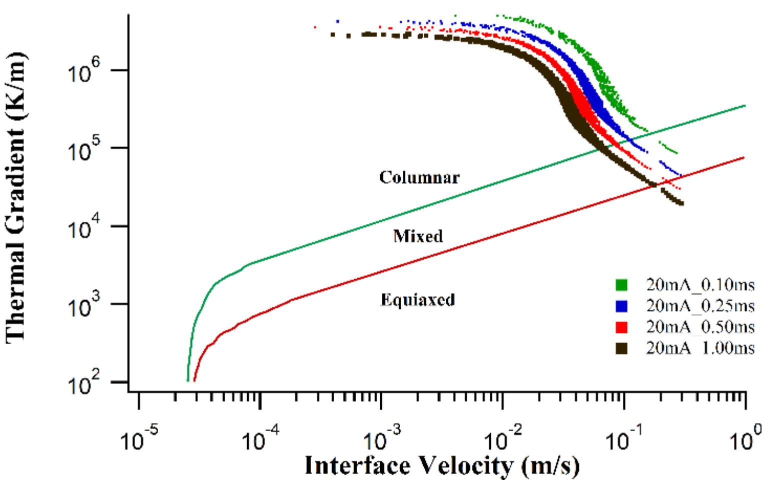

c) Beam ON time

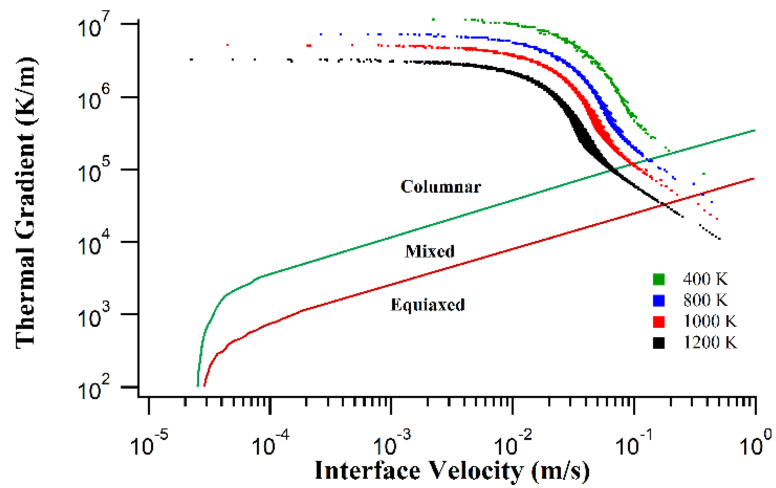

d) Preheat Temperature

How can we quantify the effect?

- Calculating volume fraction of equiaxed grains as a function of G and R at each node of the spatial domain.

$$\left(\frac{G^n}{R}\right) = a\left\{\left(\frac{-4\pi N_o}{3\ ln(1-\Phi_i)}\right)^{\frac{1}{3}} \cdot \frac{1}{n+1}\right\}^n$$

$$\Phi_i = 1 - exp\left\{-2.358E18 * \left(\frac{R}{G^{3.4}}\right)\right\}^{\frac{3}{3.4}}$$

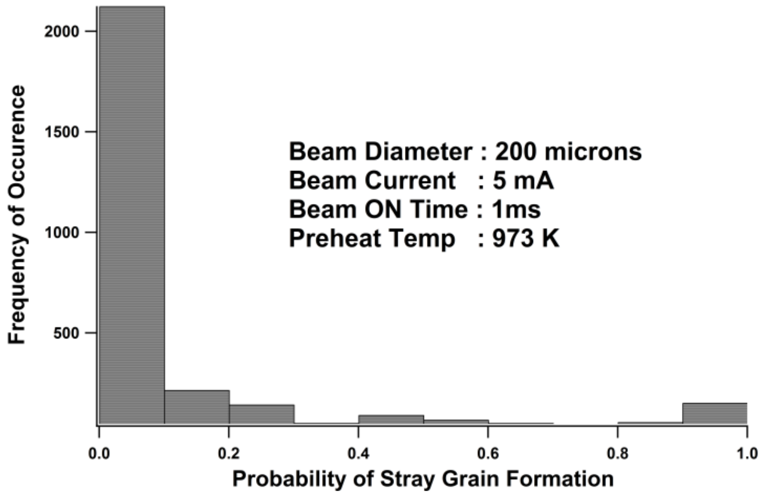

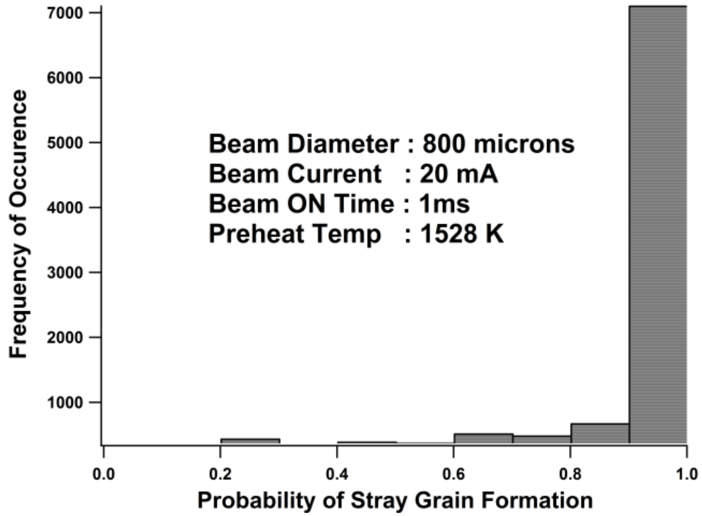

- Calculation of volume weighted average of equiaxed grains for a meltpool.

$$\boldsymbol{\Phi} = \frac{\Sigma V_i \boldsymbol{\Phi}_i}{\Sigma V_i}$$

Statistical Analysis To Identify Significance of Process Parameters

Parameter	Minimum	Maximum
Electron beam Diameter FWHM (μ)	200	800
Electron beam current (mA)	5	20
Spot ON time (ms)	0.1	1
Preheat temperature (K)	973	1528

Input parameter ranges considered for simulations

Case #	A Beam Diameter (μ)	B Beam Current (mA)	C Spot ON time (ms)	D Preheat Temperature (K)	Response Variable Φ (%)
1	200	5	0.1	973	13.7
2	200	5	0.1	1528	57.5
3	200	5	1	973	15.9
4	200	5	1	1528	75.3
5	200	20	0.1	973	15.8
6	200	20	0.1	1528	67.8
7	200	20	1	973	20.6
8	200	20	1	1528	86.0
9	800	5	0.1	973	14.1
10	800	5	0.1	1528	58.8
11	800	5	1	973	20.4
12	800	5	1	1528	76.9
13	800	20	0.1	973	17.4
14	800	20	0.1	1528	68.2
15	800	20	1	973	22.9
16	800	20	1	1528	88.1

Volume fraction of equiaxed grains for all combinations

Source	Sum of Squares	Degrees of freedom	Mean Square	F-Value	p-value Probability > F
A- Beam Diameter	12.60	1	12.60	2.12	0.1763
B- Beam Current	183.6	1	183.6	30.85	0.0002
C- Beam On Time	538.4	1	538.4	90.45	< 0.0001
D- Preheat Temperature	11979.30	1	11979.30	2012.99	< 0.0001

Identification of significant factors through ANOVA

Experimental Validation – Significance of Initial Condition (Pre-heat)

973K preheat

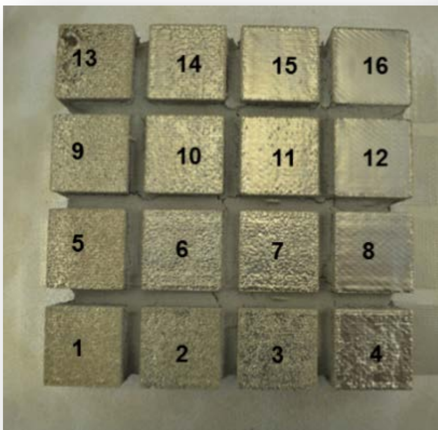

Cube Samples

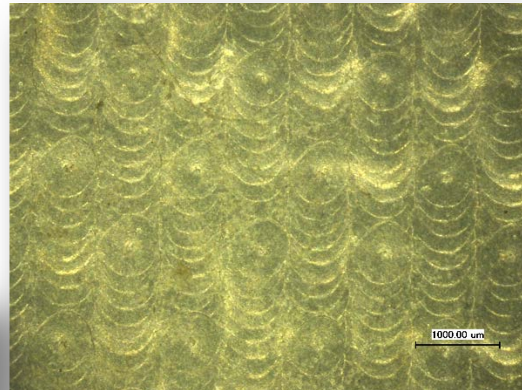

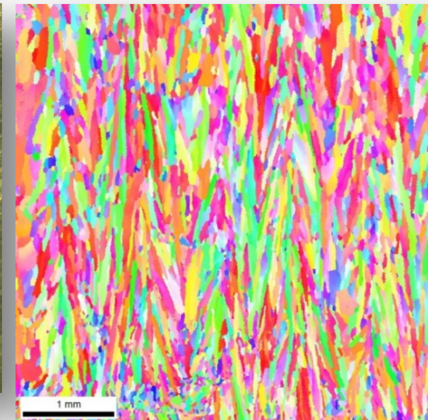

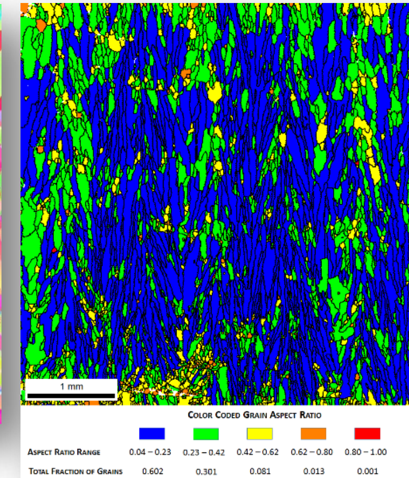

Build Direction

Top surface
melt pool effects

Crystal orientation
(EBSD – IPF)

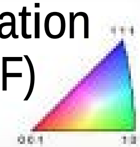

Grain aspect ratio

1528K preheat

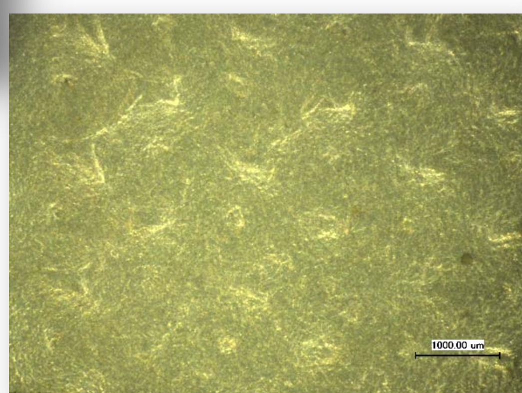

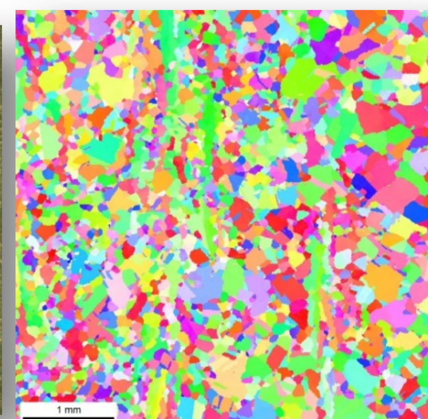

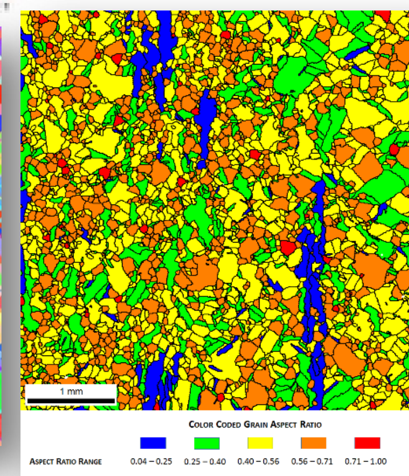

Build Direction

Recap physics and numerics needed.

Physical Processes

- Conduction
- Convection
- Thermal radiation
- Solid-solid phase transformations
- Melting and solidification
- Fluid flow with surface tension
- Solid mechanics

Numerical Methods

- Particle methods
- Viewfactor radiation
- Discrete element methods
- Phase field methods
- Finite volume methods
- Finite element methods

Tools exist that provide some combination of these capabilities, but few, if any, provide all – and even more rarely for AM processes.

Summary

- Physical processes during fusion based additive manufacturing have much in common with other manufacturing processes like casting and welding
  - Heat and mass transfer, melt/solidification, solid-state transformation, distortion and residual stress
- Efforts under way to re-purpose existing tools and develop new tools for analysis and control of powder properties and behavior
- Solid-state microstructure evolution can also be predicted by coupling overall transformation kinetics and thermal cycles.
  - We can control the extent of microstructure heterogeneity
- Control of solidification structure can be achieved by controlling temperature gradient (dT/dx) and liquid-solid-interface velocity (dx/dt) within the molten pool.

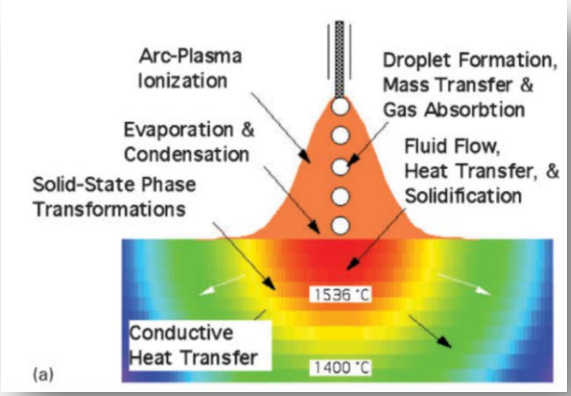

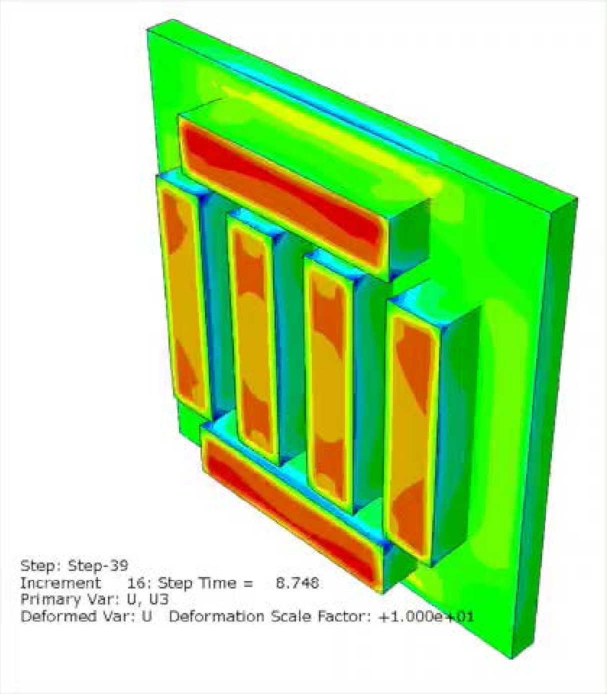

Distortion prediction in EBM process; Prabhakar et al. (2015)

Movies replaced by still image for distribution

HPC4Mfg Program
Advancing Innovation

Increase Energy Efficiency - Advance Clean Energy Technologies

- DOE/EERE Advanced Manufacturing Office (AMO)
- US Manufacturers, Universities, and supporting organizations
  - Identify industry challenge
  - Commit 20% "in kind" funding (non-gov)
  - IP Protection
  - Announce success

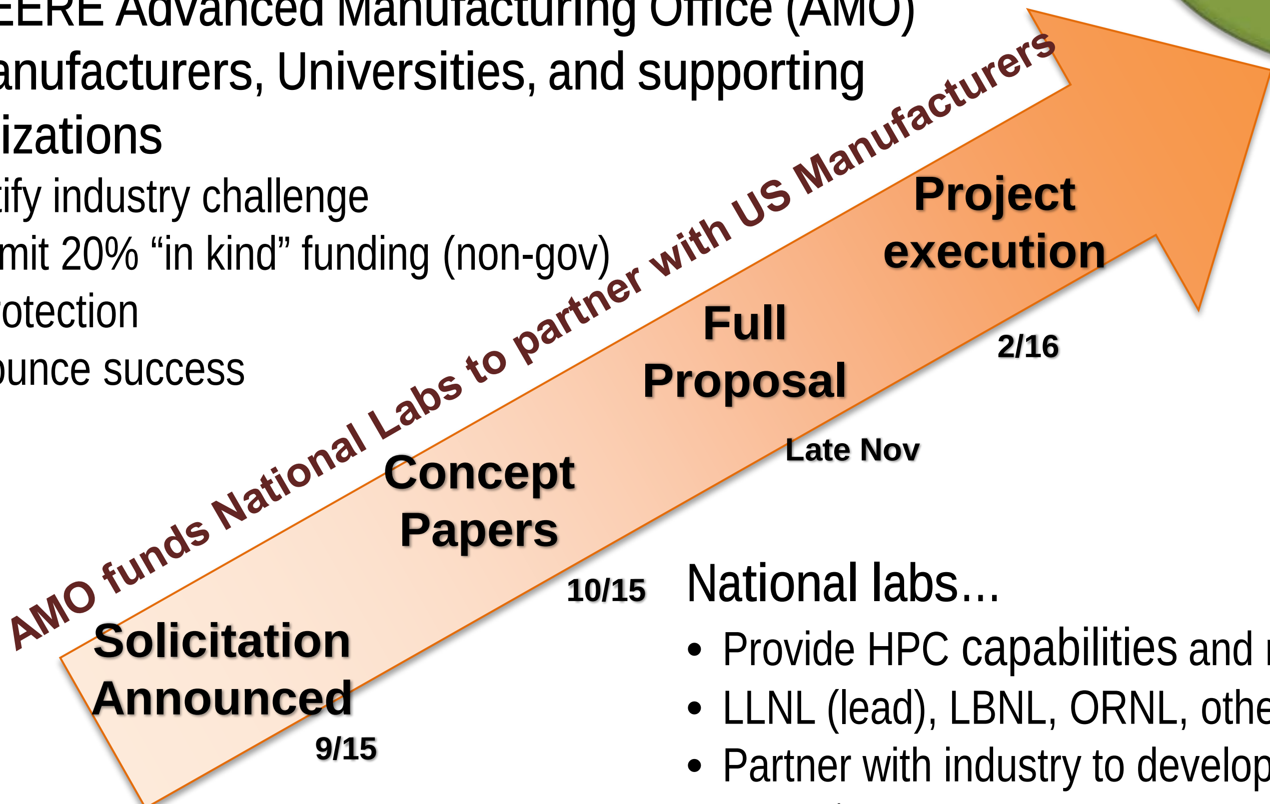

National labs…

- Provide HPC capabilities and mod / sim expertise
- LLNL (lead), LBNL, ORNL, other labs join in future calls
- Partner with industry to develop full proposal
- Up to $300k DOE funding
- Standard CRADA sympathetic to protection of IP

US Manufacturing losing market share and large energy consumer

http://hpc4mfg.llnl.gov

Questions?

e-mail: turnerja@ornl.gov

The research and activities described in this presentation were performed using the resources at Oak Ridge National Laboratory, which is supported by the Office of Science of the U.S. Department of Energy under Contract No. DE-AC0500OR22725.

OAK RIDGE National Laboratory

DOE's first Manufacturing Demonstration Facility located at ORNL

Leveraging core capabilities to support advanced manufacturing

- Neutron scattering
- High-performance computing
- Advanced materials
- Advanced characterization

U.S. DEPARTMENT OF ENERGY | Advanced Manufacturing


Hardin Valley Campus

Manufacturing Demonstration Facility (MDF): a multidisciplinary DOE-funded facility dedicated to enabling demonstration of next-generation materials and manufacturing technologies for advancing the US industrial economy

www.ornl.gov/manufacturing

The Oak Ridge Leadership Computing Facility is one of the world's most powerful computing facilities

- 27.1 PF/s peak performance
- 17.6 PF/s sustained perf. (LINPACK)
- 18,688 compute nodes, each with:
  - 16-Core AMD Opteron CPU
  - NVIDIA Tesla "K20x" GPU
  - 32 + 6 GB memory
- 710 TB total system memory
- 200 cabinets (4352 ft^2)
- 8.9 MW peak power

Spallation Neutron Source

- The ecosystem surrounding the machine – file systems, visualization resources, expertise – is where science really happens.
- Experimental validation, data analysis, and visualization are the steps in the scientific workflow that lead to insight.